

The Considère Diagram

A Review of Uniaxial Stress-Strain Relationships for Finite Deformations

Kaspar Willam, CU-Boulder

Uniaxial Tension Experiments on Metals:

For metals it is widely accepted that the stress-strain diagram is symmetric with regard to tension and compression when plotted in terms of true rather than nominal quantities. Kinematic considerations state that the engineering definition of nominal strain exhibits fundamental deficiencies under rigid body rotations and deformations which are not truly infinitesimal. For these two reasons the direct tension behavior of metals is normally plotted in science-oriented publications in terms of true rather than nominal measures of stress and strain.

In contrast, the structural engineering community prefers to plot stress-strain diagrams in terms of nominal rather than true measures of stress and strain which clearly depicts the ultimate strength of the material. There is a one-to-one relationship between true and nominal measures, hence in principle it should make little difference which representation is used to display the main features of the direct tension test. Unfortunately, the true-stress-strain diagram does not depict the point of ultimate load resistance which distinguishes hardening from softening. It is this point in the deformation history where the tangential stiffness of elastoplastic constitutive models loses positive definite properties and where the tangential localization operator indicates the formation of discontinuities e.g. in the form of shear bands (loss of ellipticity and positive wave speeds). Further, traditional finite element failure computations exhibit strong mesh sensitivity, one speaks of 'loss of mesh objectivity' if no special provisions are made to capture or regularize these discontinuities in the softening regime. In short, for failure analysis, it is the ultimate strength and the ductility which are of main interest.

For this reason it is important to locate the ultimate strength which corresponds to the point of failure initiation at the material level. Since the true stress-strain diagram exhibits hardening and does not indicate the drastic difference between hardening and softening it is proposed to combine the two representations of the uniaxial tension experiment using the '*Considère Diagram*' which superimposes the two measures of stress and strain in a single plot, see e.g. Considère [1], Nadai [2], or Meyers and Chawla [4].

1. Preliminaries:

In order to understand the construction of this stress-strain diagram, we recall the definitions of nominal and true stress and strain under uniaxial tension:

- Nominal axial stress and strain:

$$\sigma^{nom} = \frac{N}{A_o} \quad \text{and} \quad \epsilon^{nom} = \frac{L - L_o}{L_o} = \lambda - 1 \quad (1)$$

Here N denotes the normal internal force in the uniaxial tension test (where from statics $N = F$ is the external axial force), A_o designates the undeformed cross-sectional area, L , and L_o are the elongated and undeformed gauge lengths, and $\lambda = \frac{L}{L_o}$ is the axial stretch of the specimen within the gauge length.

- True axial stress and strain at failure:

$$\sigma_f^{true} = \frac{N_f}{A_f} \quad \text{and} \quad \epsilon_f^{true} = \int_{L_o}^{L_f} \frac{dL}{L} = \ln \frac{L_f}{L_o} = \ln \lambda_f \quad (2)$$

Here A_f denotes the deformed cross-sectional area and L_f the value of the deformed gauge length at failure, while L_o designates the initially undeformed gauge length.

- Incompressibility:

Assuming incompressible behavior of the dominant plastic deformations in the hardening and softening regimes, the axial stretch is related to the area reduction by:

$$dV = 0 \quad \text{leads to} \quad dAL + A dL = 0 \quad \text{or} \quad \frac{dL}{L} = -\frac{dA}{A} \quad (3)$$

Hence the true strain at failure may be expressed in terms of the reduction of the cross-sectional area and the diameter D of the cylindrical cross section,

$$\epsilon_f^{true} = \ln \frac{L_f}{L_o} = \ln \frac{A_o}{A_f} = 2 \ln \frac{D_o}{D_f} \quad (4)$$

Here D_o , D_f denote the diameters of the undeformed and the deformed specimen. Thereby it is widely accepted that the reduction of area, RA, provides an 'objective' measure of ductility as opposed to $\frac{L_f}{L_o}$ which depends on the gauge length.

$$RA = \frac{A_o - A_f}{A_o} = 1 - e^{-\epsilon_f^{true}} \quad (5)$$

Note:

The statement that metals behave symmetrically in tension and compression infers that true measures of stress and strain are used for values larger than 2% (when $\epsilon^{nom} = 0.02$

corresponds to $\epsilon^{true} = 0.0198$). Further it is understood that this statement holds only up to the point of ultimate load resistance in tension before softening takes place. Clearly, the necking region depends on the triaxial confinement when cleavage and pore-growth take place leading to 'cup-cone' rupture in tension in contrast to a 'barreling' flow mechanism in compression when short cylindrical specimens are used. Hence it is inappropriate for the necking region to determine the axial strain from,

$$\epsilon^{true} = \ln \frac{L}{L_o} = \ln(1 + \epsilon^{nom}) \quad (6)$$

In fact, the 'true' representation of the necking response requires continuous measurements of the diameter D according to Eq. 4 starting from the point of ultimate strength all the way to the point of failure.

In the light of the 'loss of mesh objectivity' of nonlinear finite element computations (when no provisions are made to capture strain localization) it is important to identify the point of ultimate load resistance which demarcates softening from hardening and the onset of necking in tension. Hence, the *Considère Diagram* is of immediate relevance since it locates the point of ultimate load resistance in the true stress - true strain diagram, see Nadai [2].

2. Considère Diagram [1]:

The onset of necking takes place when the internal force reaches a maximum value, i.e. when $\frac{dN}{dL} = 0$. Expressing the internal force in terms of nominal quantities, the point of ultimate stress is simply located at the 'peak' of the nominal stress-strain diagram where $E_{tan}^{nom} = \frac{d\sigma^{nom}}{d\epsilon^{nom}} = 0$ since $N_u = \sigma_u^{nom} A_o$ and $\epsilon_u^{nom} = \frac{dL}{L_o}$. In contrast to this simple identification of the onset of necking the point of ultimate strength can not readily be identified when plotting true quantities. In this case $N_u = \sigma_u^{true} A_u$, and the ultimate load resistance is reached when

$$\frac{dN}{dL} = \sigma_u^{true} \frac{dA}{dL} + A_u \frac{d\sigma^{true}}{dL} = 0 \quad (7)$$

Considering the incompressibility condition in Eq. 3, which states that $\frac{dA}{dL} = -\frac{A_u}{L_u}$ at the ultimate value of true stress, the tangent modulus of the true stress - true strain diagram must satisfy the condition,

$$\frac{d\sigma^{true}}{d\epsilon^{true}} = \sigma_u^{true} \quad (8)$$

This infers that the peak strength is located at that point where the tangent of the true stress - true strain diagram, $E_{tan}^{true} = \frac{d\sigma^{true}}{d\epsilon^{true}}$ coincides with the secant value, $E_{sec} = \frac{\sigma^{true}}{\epsilon}$ as shown in Fig. 1.

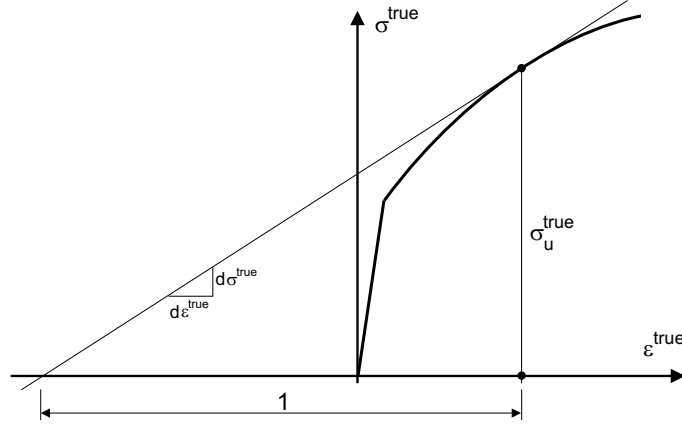


Figure 1: True-Stress-Strain Relation at Point of Ultimate Strength

On the other hand, the true stress is related to the nominal stress at the ultimate nominal strain as follows,

$$\sigma_u^{true} = \frac{N_u}{A_u} = \frac{N_u}{A_o} \frac{A_o}{A_u} = \sigma_u^{nom} [1 + \epsilon_u^{nom}] \quad \text{where} \quad \frac{A_o}{A_u} = \frac{L_u}{L_o} = 1 + \epsilon_u^{nom} \quad (9)$$

and where the incompressibility argument was used to eliminate $\frac{A_o}{A_u}$ in Eq. 9. In other terms, the true and the nominal stress values at the point of ultimate nominal strain are related by the expression,

$$\frac{\sigma_u^{true}}{1 + \epsilon_u^{nom}} = \sigma_u^{nom} \quad (10)$$

This relationship forms the core of the '*Considère Diagram*' in which the nominal and true values of stress and strain are superimposed. Fig. 2 shows that the horizontal tangent of the nominal stress-strain diagram at the point of ultimate strength corresponds to the inclined tangent $E_{tan}^{true-nom} = \frac{\sigma_u^{true}}{1 + \epsilon_u^{nom}}$ relating the true stress to the nominal strain at the point of ultimate load resistance.

Conclusions:

In summary, the '*Considère Diagram*' helps to locate the point of ultimate strength in the true stress-strain diagram when $E_{tan}^{true} > 0$. This point corresponds to $E_{tan}^{nom} = 0$ in the nominal stress-strain diagram which demarcates hardening from softening which is responsible for the loss of positive definiteness and the formation of localized failure mechanisms particularly when loaded in shear.

Aside from the uniaxial description of the direct tension test in terms of nominal or true (natural) measures of stress and strain, it is the triaxiality which needs to be considered in the

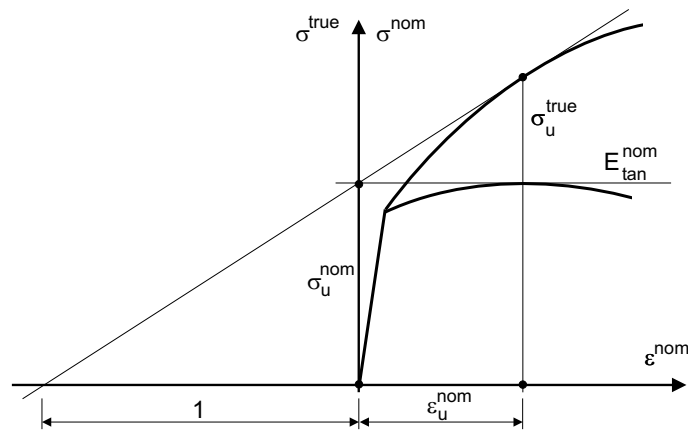


Figure 2: Considère Diagram at Point of Ultimate Strength

necking region when uniform conditions cease to exist. The curvature of the neck introduces a triaxial state of stress which was investigated by Bridgman [3] in the context of his celebrated experiments on the effect of hydrostatic stress. In fact the necking region is subject to a state of triaxial tension which tends to suppress discontinuous bifurcation in the form of localized failure modes. The recent study by Geers [5] of large deformation elasto-plastic softening sheds additional light onto the fascinating necking mechanisms behind cup-cone failure and the effect of gradients of plasticity and elastic damage on modeling softening.

References:

- (1) Considère, A., *Annales des Ponts et Chaussées*, Ser. 6, 1885, 574.
- (2) Nadai, A., *Theory of Flow and Fracture of Solids*, Vol. 1, McGraw-Hill Book Company, Inc., New York, 2nd Ed. 1950.
- (3) Bridgman, P.W., *Studies in Large Plastic Flow and Fracture*, Harvard University Press, 1964.
- (4) Meyers, M.A. and Chawla, K.K., *Mechanical Behavior of Materials*, Prentice-Hall, Inc. 1999.
- (5) Geers, M.G.D., 'Finite strain logarithmic hyperelasto-plasticity with softening: a strongly non-local implicit gradient framework', *Comp. Meth. Appl. Mech Engrg.*, Vol. 193, (2004) 3377-3401.